

Thermal Properties of Poly(ϵ -Caprolactone)/Multiwalled Carbon Nanotubes Composites

Hun-Sik Kim, Yun Seok Chae, Jae Hoon Choi, Jin-San Yoon and Hyung-Joon Jin*

Department of Polymer Science and Engineering, Inha University, 402-751 Incheon, Korea

Received 29 June 2007; accepted 10 September 2007

Abstract

In this study, multiwalled carbon nanotubes (MWCNTs) were compounded with the poly(ϵ -caprolactone) (PCL) matrix at the solution state using chloroform. For homogeneous dispersion of MWCNTs in polymer matrix, oxygen-containing groups were introduced on the surface of MWCNTs. The mechanical properties of the PCL/MWCNTs composites were effectively increased due to the incorporation of MWCNTs. The composites were characterized using scanning electron microscopy in order to obtain information on the dispersion of MWCNT in the polymeric matrix. In case of 1.2 wt% of MWCNTs in the matrix, strength and modulus of the composite increased by 12.1% and 164.3%, respectively. In addition, the dispersion of MWCNTs in the PCL matrix resulted in substantial decrease of the electrical resistivity of the composites as the MWCNTs loading was increased from 0 to 2.0 wt%. Furthermore, thermal stability of the PCL and PCL/MWCNTs-COOH composites were investigated using the data acquired from the thermogravimetric analysis. The detailed kinetics of the thermal degradation of the composites was investigated by analyzing their thermal behavior at different heating rates in a nitrogen atmosphere. Activation energy of thermal degradation was determined by using the equations proposed by Kissinger and Flynn–Wall–Ozawa. The apparent activation energy of PCL/MWCNTs-COOH composite was considerably higher than that of neat PCL.

© Koninklijke Brill NV, Leiden, 2008

Keywords

Biodegradable, multiwalled carbon nanotubes, nanocomposites, poly(ϵ -caprolactone), thermal stability

1. Introduction

Research in biodegradable polymers has gained considerable momentum in recent years due to the increasingly attractive environmental, biomedical and agricultural applications [1, 2]. Therefore, poly(ϵ -caprolactone) (PCL) is widely used in medical applications such as surgical implants [3], tissue culture [4], resorbable sutures [5], wound closure and controlled release systems [6].

* To whom correspondence should be addressed. E-mail: hjjin@inha.ac.kr
Edited by the KSCM

Carbon nanotubes (CNTs) are one of the most promising candidates for the design of novel ultrahigh strength polymer composites [7–9]. It is believed that the high aspect ratio, mechanical strength, and electrical and thermal conductivity of CNTs can enhance the overall performance of many polymer–CNTs composites and open up new applications [10, 11]. Polymer/CNTs composites are easily molded and the resulting shaped plastic articles have a perfect surface appearance compared with the polymer composites made using conventional carbon or glass fibers. Good interfacial adhesion between the CNTs and the polymer matrix is essential for efficient load transfer in the composite. These novel ultrahigh strength polymer composites demand uniform dispersion of the CNTs in the polymer matrix without their aggregation and, therefore, a strong CNTs/polymer matrix interaction is needed. So far, the potential benefits of CNTs have not been fully taken advantage of, due to the difficulties involved in producing polymer/CNTs composites with well-dispersed CNTs. Both noncovalent and covalent modifications of the CNTs surface have been used to improve the wettability and solubility of CNTs. The noncovalent approach includes surfactant modification, polymer wrapping and polymer absorption. The advantage of noncovalent attachment is that the perfect structure of the CNTs is not damaged and, consequently, their mechanical properties remain intact [12, 13]. Multifunctional polymer/CNTs composites are also under development, where in addition to improved mechanical properties, increases in electrical conductivity and improved thermal properties are obtained with small amounts of embedded CNTs [14].

In this study, the mechanical properties of PCL were improved by the incorporation of MWCNTs into PCL through the solution blending method. In addition, the morphological and electrical properties of the PCL/MWCNT composites were investigated. Furthermore, we attempted to obtain the activation energy of thermal degradation by means of thermogravimetric analysis (TGA). The thermal degradation behavior provides useful information which can be used for the establishment of the optimum processing conditions as well as to identify the potential applications of the materials [15]. The detailed kinetics of the thermal degradation of the composites was investigated by analyzing their thermal behavior at different heating rates in a nitrogen atmosphere.

2. Experimental

2.1. Materials

A commercially available PCL was supplied by Union Carbide Co., USA with a molecular weight of 1.6×10^5 g/mol. The MWCNTs (Iljin Nanotech Co., Korea) synthesized by a thermal chemical vapor deposition method was used. Purity of the MWCNTs was >95%. Chloroform was obtained from Aldrich and used as received.

2.2. Purification of MWCNTs

To eliminate the impurities in the MWCNTs (such as metallic catalysts), they were treated in a mixture of 3 M HNO₃ and 1 M H₂SO₄ at 60°C for 12 h, followed by refluxing in 5 M HCl at 120°C for 6 h. The purity of the acid-treated MWCNTs was measured to be 99% using thermogravimetric analysis (TGA, Q50, TA instruments, UK). These acid-treatments are known to introduce carboxylic and hydroxyl functional groups onto the surface of the MWCNTs [16, 17]. The functionalized MWCNTs were filtered and washed with a large amount of water and then vacuum-dried at room temperature overnight.

2.3. Preparation of PCL/MWCNT Composites

A 250 ml flask charged by predetermined content of the MWCNTs (MWCNTs and MWCNTs-COOH, respectively), 5.0 g of PCL and 100 ml of CHCl₃ was sonicated in a bath (40 kHz) for 30 min. The mixture was then dried under convection oven for 24 h at room temperature. The PCL/MWCNT composites were compression molded in the module with 0.3 mm thickness at 120°C and the pressure of 1 ton was applied using a Carver laboratory press. From these laminates, the specimens used for the mechanical tests were obtained according to the ASTM D 638 standard.

2.4. Characterization

The functionalization on the surface of the MWCNTs was analyzed by Fourier transformed infrared spectroscopy (FT-IR, Perkin-Elmer, Spectrum 2000, USA). The morphology of the liquid nitrogen fractured surfaces was investigated using a scanning electron microscope (SEM, S-4300, Hitachi, Japan). The fractured samples were coated with a homogenous Pt layer by using an ion sputter (E-1030, Hitachi, Japan). The SEM images were collected at an accelerating voltage of 15 kV. The electrical conductivity of the composites was determined by measuring the volume resistivity (Ω cm), which is a value of the resistance expressed in a unit volume by a 2-probe method. The value is an absolute value specific to the material and is determined by measuring the potential difference (V) between the two electrodes separated in a distance (L) when the constant current I (A) flows through the cross-sectional area $W \times t$. The thermal properties of the PCL and PCL/MWCNT composites were investigated using TGA by scanning from 30 to 700°C at heating rates of 5, 10, 20, 40°C/min under nitrogen atmosphere. The thermal stability of the composites was determined from the thermogram of TGA.

3. Results and Discussion

The mechanical properties of PCL were enhanced by the incorporation of various contents of MWCNTs by solution compounding. The well-dispersed MWCNT in PCL matrix was observed by SEM because some content of carboxylic acid groups were introduced onto the walls or ends of individual MWCNTs (MWCNT-COOH) during the purification step, which were compatible with PCL. Figure 1 shows the

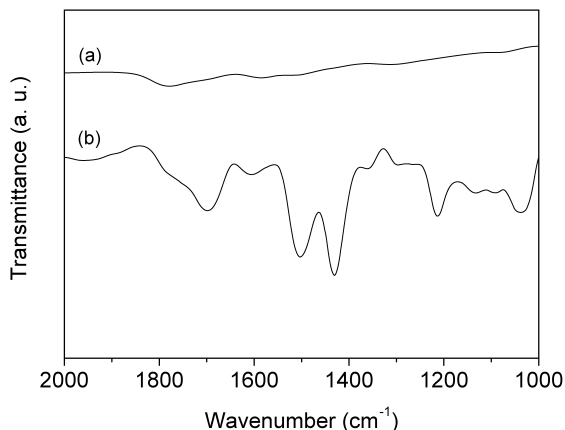


Figure 1. FT-IR spectra of (a) MWCNT and (b) MWCNT-COOH.

Table 1.

Mechanical properties of PCL and PCL/MWCNT composites at the same contents (1.2 wt%) of MWCNTs

Sample	Tensile stress (MPa)	Young's modulus (MPa)
PCL	17.3 ± 1.2	355.7 ± 53.6
PCL/MWCNT	16.7 ± 0.5	662.5 ± 28.4
PCL/MWCNT-COOH	19.4 ± 0.4	940.1 ± 30.3

FT-IR spectra of MWCNT and the MWCNT-COOH. The FT-IR spectrum of the MWCNT-COOH exhibits the C=O stretching at 1705 cm^{-1} corresponding to the carboxyl groups while the same peak was not observed in the MWCNT.

PCL/MWCNT and PCL/MWCNT-COOH composites were prepared for tensile test. It was performed to evaluate the effect of functionalized MWCNT on the mechanical properties of the composites. The addition of MWCNT-COOH (1.2 wt%) to PCL increased the tensile strength and modulus by 12.1% and 164.3%, respectively, as shown in Table 1 and Fig. 2. The elongations at break of the PCL matrix and PCL/MWCNT composites at all compositions are higher than 500%. The Young's modulus of PCL matrix was remarkably enhanced by the incorporation of a small amount of MWCNT-COOH (1.2 wt%), which was more effective than when MWCNT was incorporated in composites. Note that mechanical properties of the composite depend on the dispersity of reinforcements in matrix [18].

Figure 3 compared SEM images of PCL/MWCNT and PCL/MWCNT-COOH composites at the same contents of MWCNTs. Figure 3(a) shows that, in the case of PCL/MWCNT composites, much of the MWCNT were aggregated in the PCL matrix. However, Fig. 3(b) shows that a substantial amount of MWCNT appears to be well dispersed and embedded in the PCL matrix.

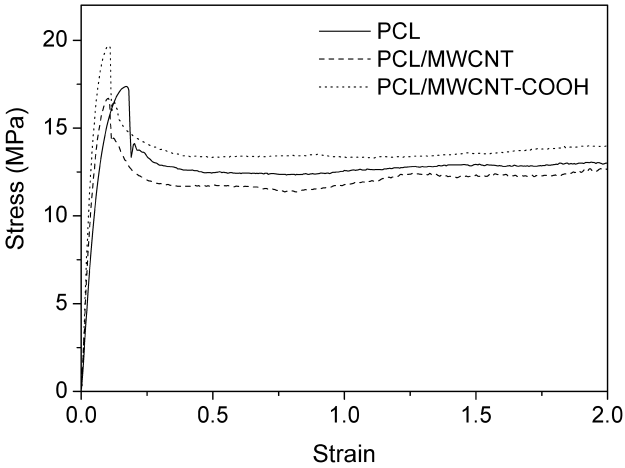


Figure 2. The representative stress–strain curves of PCL, PCL/MWCNT (1.2 wt%) and PCL/MWCNT-COOH (1.2 wt%) composites.

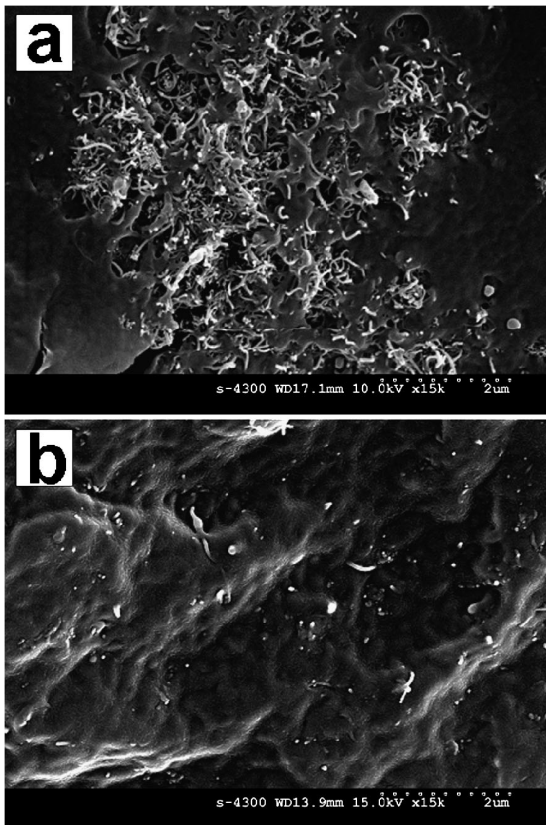


Figure 3. SEM images of the fractured surface of (a) PCL/MWCNT, (b) PCL/MWCNT-COOH composites at same contents (1.2 wt%) of MWCNTs.

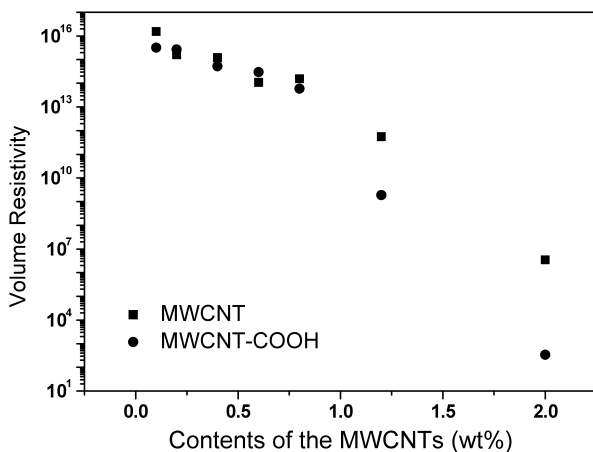


Figure 4. Volume resistivity of PCL/MWCNT and PCL/MWCNT-COOH composites at various contents of MWCNT.

Table 2.

$T_{5\%}$ and $T_{50\%}$ values PCL, PCL/MWCNT (1.2 wt%) and PCL/MWCNT-COOH (1.2 wt%) composites determined from TGA

Heating rate (°C/min)	PCL		PCL/MWCNT		PCL/MWCNT-COOH	
	T_5 (°C)	T_{50} (°C)	T_5 (°C)	T_{50} (°C)	T_5 (°C)	T_{50} (°C)
5	361.3	397.8	363.5	397.3	364.0	399.3
10	378.4	415.1	380.3	415.9	380.8	418.7
20	397.8	434.6	400.2	436.1	404.3	437.6
40	418.9	457.6	423.7	460.4	427.5	465.8

The volume resistivity of the composites was measured by a two-probe method at room temperature and compared as shown in Fig. 4. The dispersion of MWCNTs in the PCL matrix resulted in substantial decrease in the electrical resistivity of the composites as the functionalized MWCNTs loading was increased. Especially, the electrical resistivity of the composites decreased over eleven orders of magnitude from 10^{13} to 10^2 Ω cm as the content of the MWCNTs-COOH increased from 0.8 to 2.0 wt%.

Two parameters, namely, the temperature corresponding to a weight loss of 5 wt% ($T_{5\%}$) and that corresponding to a weight loss of 50 wt% ($T_{50\%}$), both measured at different heating rates, are listed in Table 2. In sharp contrast, the $T_{5\%}$ and $T_{50\%}$ values of the PCL/MWCNT-COOH composites were raised when they were compared with those of PCL matrix. In order to examine closely the curious thermal degradation behavior of PCL/MWCNT-COOH composites, activation energies of thermal degradation were measured using the corresponding TGA data. According to the Kissinger method [19] in equation (1), the activation energy can

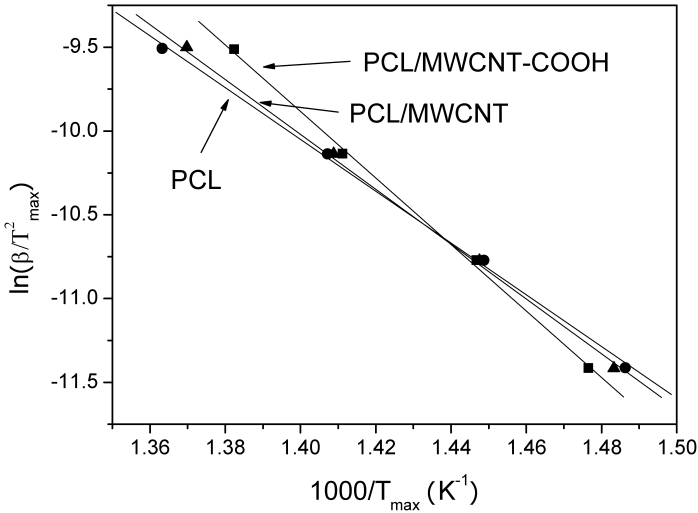


Figure 5. The plots used for the determination of the activation energies of PCL, PCL/MWCNT (1.2 wt%) and PCL/MWCNT-COOH (1.2 wt%) composites according to the Kissinger’s method.

be determined from the slope of the plot of $\ln(\beta/T_{\max}^2)$ versus $1/T_{\max}$, which is exemplified in Fig. 5.

$$\ln \frac{\beta}{T_{\max}^2} = \left\{ \ln \frac{AR}{E} + \ln[n(1 - \alpha_{\max})^{n-1}] \right\} - \frac{E}{RT_{\max}}, \quad (1)$$

where β is the heating rate, T_{\max} is the temperature corresponding to the inflection point of the thermal degradation curves at the maximum degradation rate, A is the pre-exponential factor, α_{\max} is the maximum conversion and n is the reaction order. The peak temperature (T_{\max}) is determined from the differential TGA curves. The activation energy, E , can be calculated from the slope of $\ln(\beta/T_{\max}^2)$ as a function of $1/T_{\max}$.

The activation energy can also be determined by using the Flynn–Wall–Ozawa method [20, 21] as shown in equation (2):

$$\log \beta = \left[\log \left(\frac{AE}{R} \right) - \log f(\alpha) - 2.315 \right] - 0.4567 \frac{E}{RT}. \quad (2)$$

This is based on the integral method and the activation energy can be determined without any knowledge of reaction order. The activation energy at a given conversion can be obtained from the plot $\log \beta$ versus $1/T$ (Fig. 6). The determined activation energies are compiled in Table 3.

Both the Kissinger equation and the Flynn–Wall–Ozawa method predicted the activation energies decreasing in the order of: PCL/MWCNT-COOH composites > PCL/MWCNT composites > PCL. The increased thermal stability of the PCL/MWCNT-COOH composite compared with that of the PCL/MWCNT com-

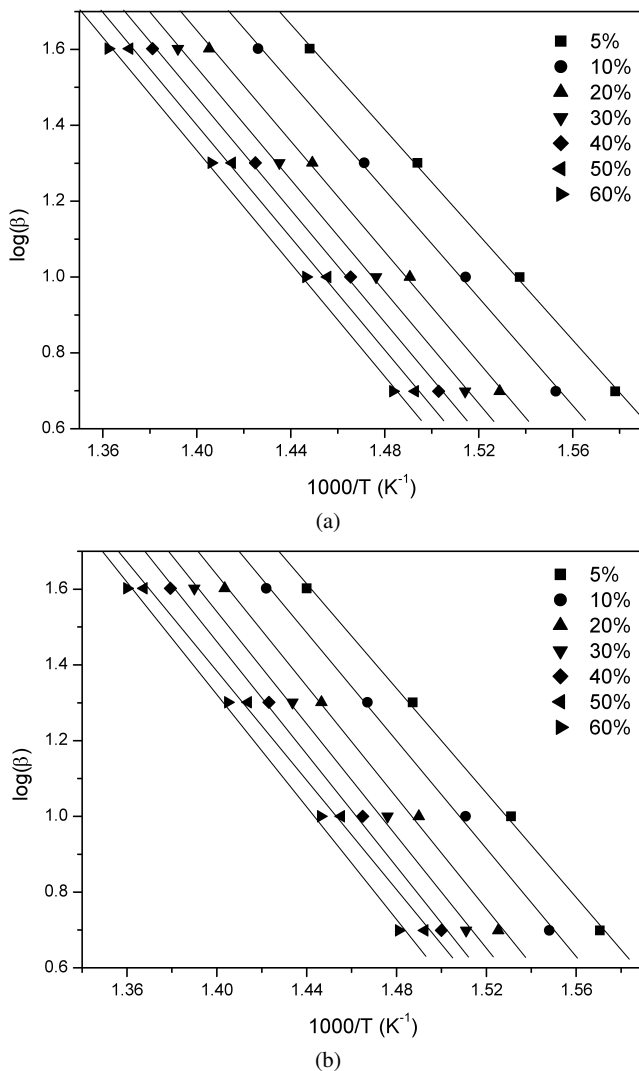


Figure 6. The plots used for the determination of the activation energies of (a) PCL, (b) PCL/MWCNT (1.2 wt%) and (c) PCL/MWCNT-COOH (1.2 wt%) composites according to the Ozawa's method.

posite is attributed to the more effective thermal shielding effect due to the dispersity of the MWCNTs-COOH. Admitting that the composite with higher activation energy is more thermally stable, these results are in line with those of the $T_{5\%}$ and $T_{50\%}$ values summarized in Table 2. Both the Kissinger and the Flynn–Wall–Ozawa methods predicted that the activation energies would be increased when the MWCNT-COOH was incorporated in the PCL matrix.

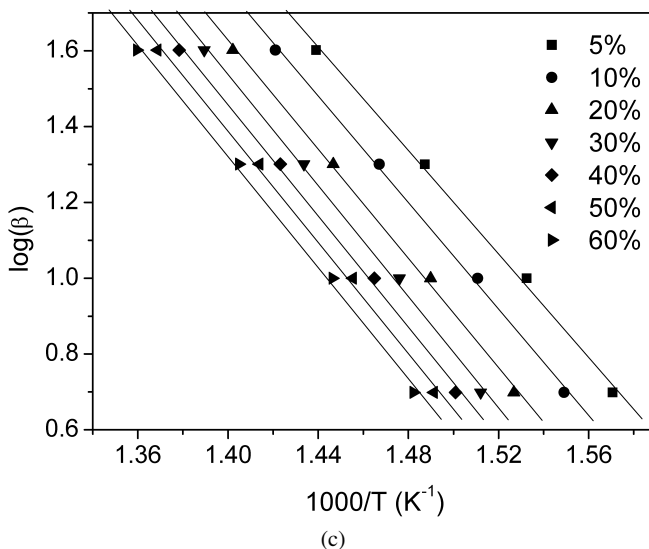


Figure 6. (Continued.)

Table 3.

Activation energy (kJ/mol) of the thermal degradation of the PCL PCL/MWCNT (1.2 wt%) and PCL/MWCNT-COOH (1.2 wt%) composites

Sample	Kissinger's method	Ozawa's method (mean value)
PCL	130.5	131.8
PCL/MWCNT	141.1	139.4
PCL/MWCNT-COOH	165.0	168.2

4. Conclusions

In this study, low contents of MWCNTs (1.2 wt%) in the composite improved the mechanical and electrical properties and thermal stability of PCL. The dispersity of MWCNTs is one of the most important factors for enhancing the mechanical and electrical properties of the composite. The electrical resistivities of the pure PCL matrix and PCL/MWCNT-COOH composites (2.0 wt%) were $2.2 \times 10^{16} \Omega \text{ cm}$ and $3.3 \times 10^3 \Omega \text{ cm}$, respectively. In addition, PCL/MWCNT-COOH composites exhibit abrupt decrease (almost eleven orders) as the MWCNT content increased from 0.8 to 2.0 wt%. It is believed that functionalized MWCNTs (MWCNT-COOH) were suitable reinforcements to enhance the electrical conductivity of PCL/MWCNT composites. Also, the mechanical properties of the PCL/MWCNT-COOH composites were effectively increased due to the well dispersed and embedded MWCNTs in the matrix. The activation energy predicted by both the Kissinger and the Flynn–Wall–Ozawa method was increased by the incorporation of MWCNT-COOH in the PCL matrix. It is believed that the MWCNT-COOH is a suitable reinforcement to

enhance the thermal stability of PCL, when it is homogeneously dispersed in the matrix polymer.

Acknowledgements

The authors of this paper would like to thank the Korea Science and Engineering Foundation (KOSEF) for sponsoring this research through the SRC/ERC Program of MOST/KOSEF (R11-2005-065).

References

1. Y. Ikada and H. Tsuji, *Macromol. Rapid Commun.* **21**, 117–132 (2000).
2. M. Malinconico, B. Immirzi, S. Massenti, F. P. La Mantia, P. Mormile and L. Petti, *J. Mater. Sci.* **37**, 4973–4978 (2002).
3. R. A. Jain, *Biomaterials* **21**, 2475–2490 (2000).
4. H. J. Jin, M. O. Hwang, J. S. Yoon, K. H. Lee, I. J. Chin and M. N. Kim, *Macromol. Res.* **13**, 73–79 (2005).
5. M. S. Taylor, A. U. Daniels, K. P. Andriano and J. Heller, *J. Appl. Biomater.* **5**, 151–157 (1994).
6. T. G. Park, S. Cohen and R. Langer, *Macromolecules* **25**, 116–122 (1992).
7. S. R. C. Vivekchand, L. Sudheendra, M. Sandeep, A. Govindaraj and C. N. R. J. Rao, *Nanosci. Nanotechnol.* **2**, 631–651 (2002).
8. G. X. Chen, H. S. Kim, B. H. Park and J. S. Yoon, *Polymer* **47**, 4760–4767 (2006).
9. M. Kang, S. J. Myung and H. J. Jin, *Polymer* **47**, 3961–3966 (2005).
10. G. X. Chen, H. S. Kim, B. H. Park and J. S. Yoon, *Carbon* **44**, 3348–3352 (2006).
11. S. R. C. Vivekchand, L. Sudheendra, M. Sandeep, A. Govindaraj and C. N. R. J. Rao, *Nanosci. Nanotechnol.* **2**, 631–635 (2002).
12. P. Pötschke, A. R. Bhattacharyya and A. Janke, *Polymer* **44**, 8061–8069 (2003).
13. C. Wei, D. Srivastava and K. Cho, *Nano Lett.* **2**, 647 (2002).
14. H. S. Kim, B. H. Park, J. S. Yoon and H. J. Jin, *Eur. Polym. J.* **43**, 1729–1735 (2007).
15. G. Sivalingam, S. P. Vijayalakshmi and G. Madras, *Indian Engng Chem. Res.* **43**, 7702–7709 (2004).
16. H. Kong, C. Gao and D. Yan, *Macromolecules* **37**, 4022–4030 (2004).
17. H. S. Kim, B. H. Park, J. S. Yoon and H. J. Jin, *Key Engng Mater.* **326–328**, 1785–1788 (2006).
18. J. Gao, M. E. Itkis, A. Yu, E. Bekyarova, B. Zhao and R. C. Haddon, *J. Amer. Chem. Soc.* **127**, 3847–3854 (2005).
19. H. E. Kissinger, *Anal. Chem.* **29**, 1702–1706 (1957).
20. T. Ozawa, *Bull. Chem. Soc. Japan* **38**, 1881–1886 (1965).
21. J. H. Flynn and L. A. Wall, *J. Polym. Sci. Part B, Polym. Letts* **4**, 323–328 (1966).